Lattice-dynamical study of impurity modes in mixed cuprous halides

P. Plumelle, D. N. Talwar,* and M. Vandevyver
Centre d'Etudes Nucléaires de Saclay, Services d'Electronique de Saclay, Laboratoire d'Etudes et de Recherches Avancées, Boîte Postale No. 2, 91190 Gif-sur-Yvette, France

K. Kunc† and M. Zigone
Laboratoire de Physique des Solides, Université de Paris VI, 4 Place Jussieu F 75230, Paris Cedex 05, France
(Received 10 April 1978; revised manuscript received 12 February 1979)

A theoretical study of impurity modes in mixed cuprous halides ($CuA_{1-x}B_x$ with A,B = Cl, Br, and I) in the low-concentration limit ($x \ll 1$) is reported using the Green's-function technique. The perturbation caused by the halogen impurity B on the phonon spectra of CuA is accounted for in terms of mass change at the impurity site as well as the change in the nearest-neighbor impurity-lattice interaction. The involved lattice Green's functions have been computed by incorporating the phonons generated by an 11-parameter rigid-ion-model fit to the recent neutron data. We find that different substitutional impurities in cuprous halides may give rise to well defined symmetry vibrations both in and outside the band-mode region. The possibility is pointed out for some of the important cases to be observed by (ir or Raman) experimental techniques. In the cases of known experimental data, we have determined the force perturbation describing the impurity-host bonding in terms of our one-parameter model. The calculated force-constant changes, in particular for Cu*Cl*:Br and Cu*Cl*:I systems, are similar to some extent to the behavior noticed in alkali halides rather than in II-VI and III-V compounds. In view of the insufficient experimental data, the possibility of the size effect cannot be ruled out. However, more experimental data on isoelectronic substituents in cuprous halides are very much needed to arrive at a general conclusion regarding the trend of force-constant change with the size of the impurity atom.

I. INTRODUCTION

CuCl, CuBr, and CuI have attracted a great deal of experimental and theoretical attention during the last decade.[1-21] Raman-scattering,[1-8] ir absorption,[9-12] neutron-scattering,[13-17] electro-optical, piezoelectric, photoelastic, x-ray diffraction,[18-19] and thermal studies[20,21] revealed that cuprous halides show anomalous behavior in their physical properties. They exhibit large ionic conductivities, and the thermal vibrations of Cu atoms are enhanced anomalously with increasing temperature.[22-25]

This series of I-VII crystals normally occurs with tetrahedral coordination as cubic zinc-blende systems (ZBS); however, they may undergo phase transition to wurtzite and rock-salt structures.[16] Indeed, their respective ionicities of 0.746, 0.735, and 0.692 are very close to the value $f_i = 0.785$ given by Phillips[26] as the limit between the groups of tetrahedrally and octahedrally coordinated compounds: This borderline situation makes the investigation of cuprous halides more interesting as it will be generally desirable to understand how far these are analogous to more ionic (I-VII) alkali halides—a group to which they belong according to their chemical composition and/or to what extent they are similar to more covalent II-VI and III-V compounds—the groups to which they belong owing to their crystal structure.

All studies involving one way or another the interatomic forces have argued that anharmonic effects in cuprous halides are predominant at room temperature. On the contrary, it is to be noted that the recent low-temperature neutron measurements of phonon dispersion for CuCl (4.2 °K)[17] and CuBr (77 °K)[16] which show no apparent anomalies, are remarkably different from the earlier results at room temperature[14,15] and are quite similar to the phonon dispersions of other ZBS compounds. This suggests a possibility to analyze the new data in terms of simple lattice-dynamical models and to evaluate them in the context of other ZBS crystals of II-VI and III-V compounds. Another source of information regarding the lattice dynamics is produced by recent Raman-scattering experiments[27] on mixed cuprous halides ($CuA_{1-x}B_x$ with A,B = Cl, Br, and I). This has shown the occurrence of localized (Cu*Br*:Cl, Cu*I*:Cl) and gap (Cu*Cl*:Br, Cu*Cl*:I) modes in the ($x \ll 1$) low-concentration limit. These kinds of data, expressed in terms of the perturbed interatomic bonding, could reveal some analysis with either rock-salt or ZBS behavior: It is known that isoelectronic impurities exhibit size effect[28] in highly ionic crystals (alkali halides) whereas no definite correlation with the ionic radii and the change in force constants was found in partially ionic crystals (II-VI and III-V compounds).[29,30]

 © 1979 The American Physical Society

In the present paper, we are attempting a lattice-dynamical study of phonons and localized vibrations in cuprous halides. Starting with a brief summary of the Green's-function theory for defect properties, we establish in Sec. II A the 11-parameter rigid-ion model (RIM 11) for CuCl and CuBr, which give good account of phonon dispersion at low temperature. After including the results of existing RIM 11 for CuI, we have completed a systematic description of the lattice dynamics of this series. In Sec. II C, a simple defect model is applied that describes the perturbed bonding in terms of a single parameter. By incorporating the defect model, the existing experimental data are interpreted and the possibility of observing new impurity modes is predicted (Sec. II D). The impurity induced in band absorption is finally calculated for heavy impurities, which may encourage experimentalists to detect it by ir techniques. This work should complete our previous study on II-VI and III-V compounds and provide us with a complete picture of impurity bonding in the isoelectronic tetrahedrally coordinated $A^N B^{8-N}$ semiconductors.

II. THEORETICAL BACKGROUND

In the Green's-function theory, the necessary condition for the existence of impurity modes (localized, gap, and resonance) is that the real part of the secular determinant vanishes,[31(a)] i.e.,

$$\mathrm{Re}\det(I - g\delta l) = 0\,, \tag{1a}$$

where g and δl are the Green's-function matrix of the perfect lattice and the perturbation matrix in the impurity space (i.e., the space directly affected by the introduction of the impurity), respectively.

The localized or gap mode frequencies appear in the region of zero density of phonons: These modes do not propagate through the crystal and are observable as δ-function peaks in optical measurements. Again, it may happen that the solution of Eq. (1a) appears at frequencies ω_R where the density of phonons is nonzero; consequently the corresponding in band mode can decay into the band continuum and acquires a width[31(d)]

$$\Gamma = 2\left|\frac{\mathrm{Im}\det(I - g\delta l)}{\dfrac{d}{d\omega^2}\mathrm{Re}\det(I - g\delta l)}\right|_{\omega^2=\omega_R^2}. \tag{1b}$$

The solutions of Eq. (1a) for which $\Gamma \ll \omega_m^2$ is also satisfied give rise to true resonant (observable) states (where ω_m is the width of the frequency spectrum of the unperturbed host crys-

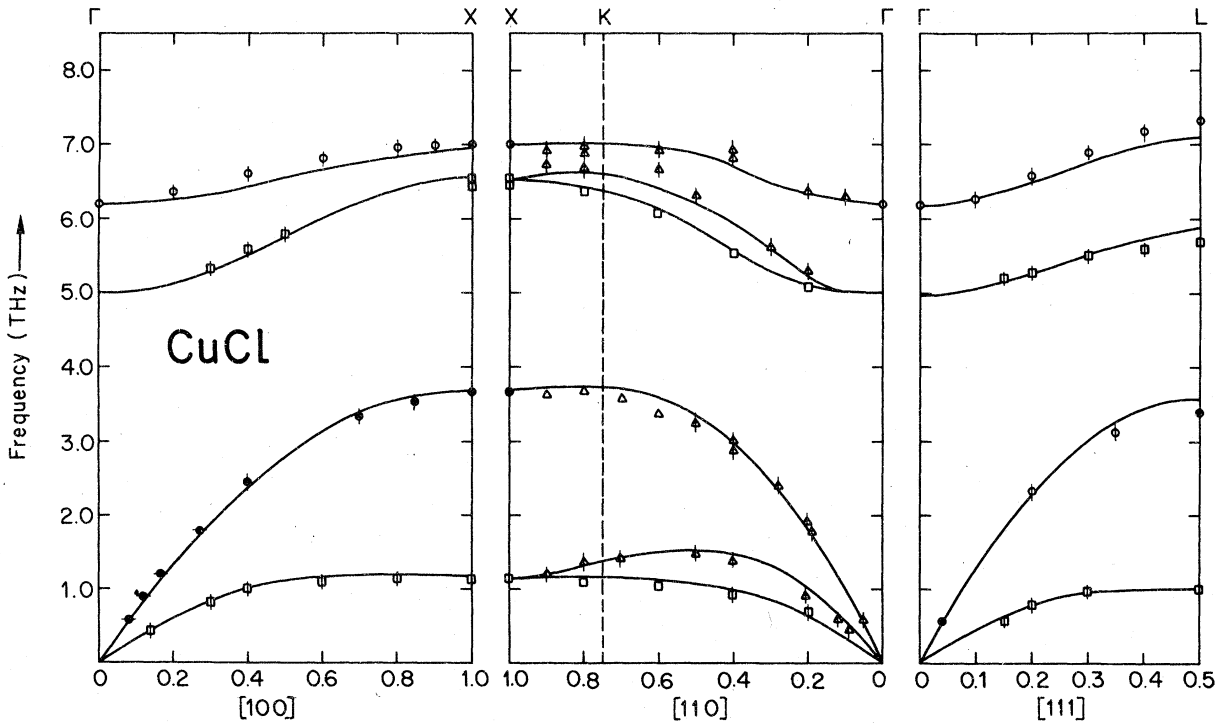

FIG. 1. Comparison of the dispersion curves (full lines) along high-symmetry directions for CuCl calculated by RIM 11 with the recent neutron data (Ref. 17).

TABLE I. Calculated model parameters (10^5 dyn cm^{-1}) for the lattice dynamics of CuCl and CuBr. The lattice parameter a_0 is in Å.

	Model parameters	
	CuCl	CuBr
a_0	2.705	2.845
A	− 0.11	− 0.1148
B	− 0.145	− 0.134
C_1	− 0.0385	− 0.0235
D_1	− 0.0253	− 0.0268
E_1	+ 0.013	+ 0.02
F_1	− 0.22	− 0.028
C_2	− 0.0035	− 0.014
D_2	− 0.0082	− 0.013
E_2	+ 0.024	+ 0.0265
F_2	+ 0.0229	+ 0.0378
z	0.5283	0.5846
M_1	35.457 (u)	63.54 (u)
M_2	63.54 (u)	79.916 (u)

tal). This rules out most of the solutions close to a maximum of the density of phonons.

A. Dynamics of perfect lattice

The evaluation of Green's functions requires a knowledge of detailed phonon energies and eigenvectors from a reliable model of lattice dynamics. Among the various phenomenological schemes the calculation of phonon dispersion exists for CuI by an 11-parameter rigid-ion model (RIM 11)[32] and also by the 15-parameter deformation-dipole model (DDM 15).[32] The results for the 14-parameter shell model (SM 14) are also available for CuCl,[17] and CuBr.[16] It is not likely to consider double-shell-model fitted room-temperature data on CuCl,[20] owing to the strong anharmonicity. The recent neutron measurements,[16,17] however, provide considerably better account of the interatomic forces in the harmonic approximation.

In order to facilitate comparison of our results

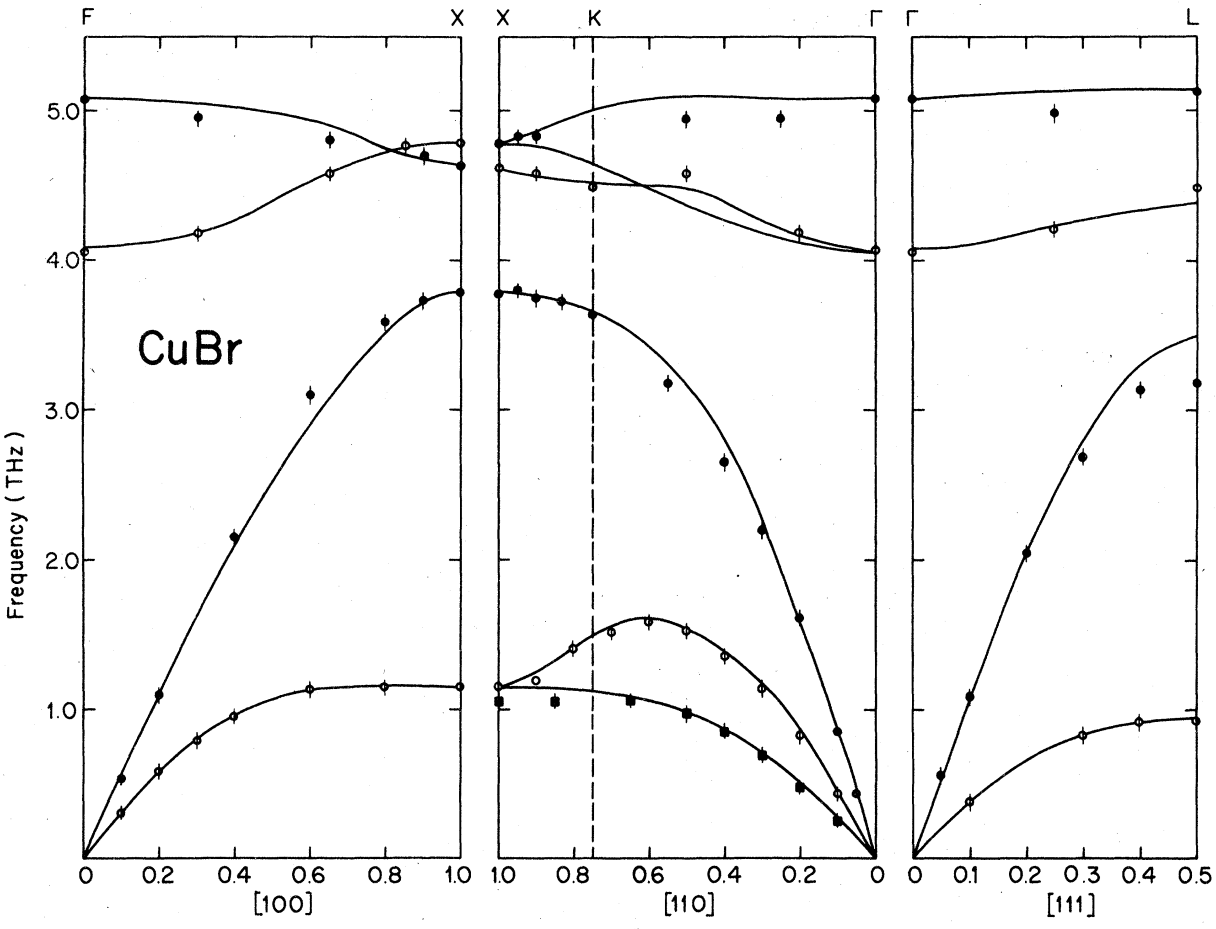

FIG. 2. Comparison of the dispersion curves (full lines) along high-symmetry directions for CuBr calculated by RIM 11 with the recent neutron data (Ref. 16).

TABLE II. Comparison of the calculated physical quantities with the experimental data for CuCl and CuBr.

Critical point	Mode	Phonon energies (cm^{-1}) CuCl Expt.[a]	CuCl Calc.	CuBr Expt.[b]	CuBr Calc.
Γ	LO	207	209	170	170
	TO	...	168	136	136
X	LO	233	232	155	155
	TO	218	218	160	160
	LA	123	123	126	126
	TA	39	39	38	38
L	LO	245	236	171	171
	TO	190	197	149	146
	LA	113	119	106	116
	TA	33	34	31	31
W	W_1	...	33		39
	W_2	...	48		52
	W_3		126		122
	W_4		218		150
	W_5		218		160
	W_6		230		166

Elastic constants (10^{11} dyn cm^{-2})	CuCl Expt.[c]	CuCl Calc.	CuBr Expt.[b]	CuBr Calc.
C_{11}	5.22[d]	5.21	4.72	4.728
C_{12}	3.49	3.49	3.72	3.72
C_{44}	1.38	1.36	1.51	1.45

[a] Reference 17.
[b] Reference 16.
[c] Reference 32.
[d] Reference 21.

with the analogous ones obtained in II-VI and III-V compounds, we consider RIM 11 for the present study. In spite of its simplicity the model is probably not completely inadequate for the description of lattice dynamics in a pronounced ionic (I-VII) compounds. We shall see that the model provides practically identical phonon dispersion as obtained by SM 14. So far as the correct prediction of eigenvectors is concerned neither of the two schemes can be judged through any of the available experimental results. It is not unlikely that even in this very ionic case the shell-model picture of interatomic interactions may be more realistic; nevertheless, we insist on the trends of various parameters, namely, the relations with defects in ZBS compounds which have been systematically treated only in terms of RIM 11. Whatever be the cases, we have noticed that RIM 11 is the only one that has provided a reasonably homogeneous set of parameters for II-VI and III-V compounds.[33-36]

The RIM 11 may be found for CuI in the work of Kunc.[32] For CuCl and CuBr, however, we have established the new set of parameters for the re-

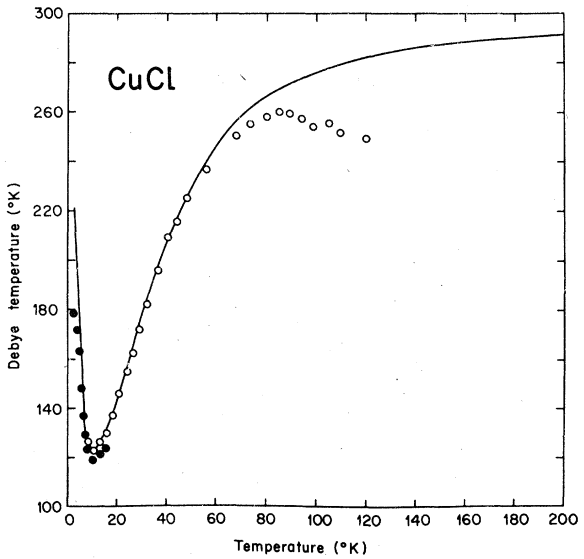

FIG. 3. Comparison of the calculated temperature for CuCl with the recent data. Full dots (●) represent the experimental results by Barron *et al.* (Ref. 21), whereas the open circles (○) represent the measurements by Vardeny *et al.* (Ref. 20).

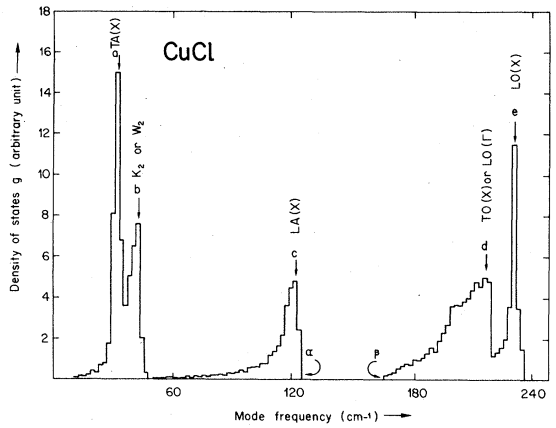

FIG. 4. Calculated one-phonon density of states g for CuCl on the basis of RIM 11 (Table III). The main peaks a, b, c, •••, e are tentatively assigned as TA(X), K_2 or W_2, LA(X), •••, LO(X). The terms α and β represent the limits of the calculated gap in the one-phonon density of state.

cent neutron data at low temperatures. The unique set of model parameters (Table I) are calculated following the procedure of Plumelle *et al.*,[37] i.e., fitting the macroscopic data first and making then the successive adjustments at the characteristic points using the least-squares method. A glance at Figs. 1 and 2 reveals that the calculated phonon dispersions along high-symmetry directions are in a satisfactory agreement with the recent neutronic results of Prevot *et al.*[17] for CuCl and of Hoshino *et al.*[16] for CuBr systems (Table II). In order to check the model parameters, we have calculated the variation of the characteristic Debye temperatures and obtained a fair agreement with the available low-temperature experimental data[20,21] (Fig. 3). Using the same model parameters we have also calculated the one- and two-phonon density of states and the results are shown in Figs. 4–9 (for the exact definitions and the normalization of g_+ and g_- we refer to the work of Kunc[32]).

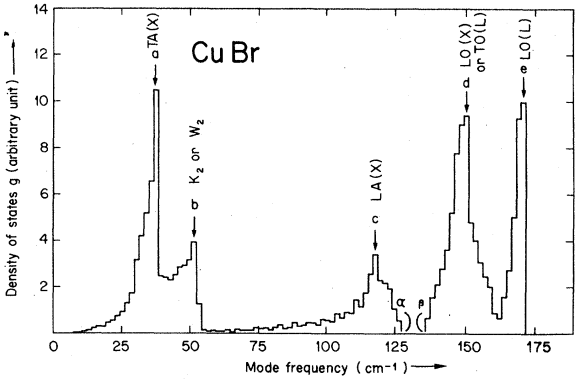

FIG. 5. Same key as Fig. 4 for CuBr.

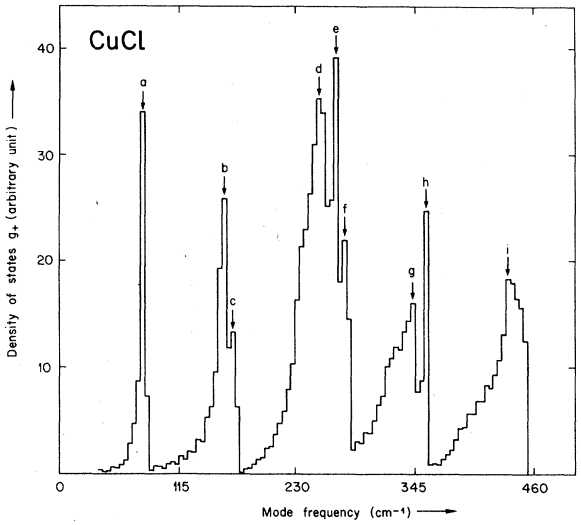

FIG. 6. The main peaks a, b, c, ..., i of two-phonon (additive) density of states (g_+) for CuCl calculated by RIM 11 are tentatively assigned using the selection rules of Birman (Ref. 40). Some of them may be compared with the two-phonon ir and Raman-scattering experimental data [Refs. 6, 10, and 12] (see Table III).

B. Analysis of the ir absorption and/or Raman-scattering spectrum of the perfect systems

In cuprous halides ir absorption and Raman-scattering experiments were performed in the past few years.[1-12] Unfortunately, the data avail-

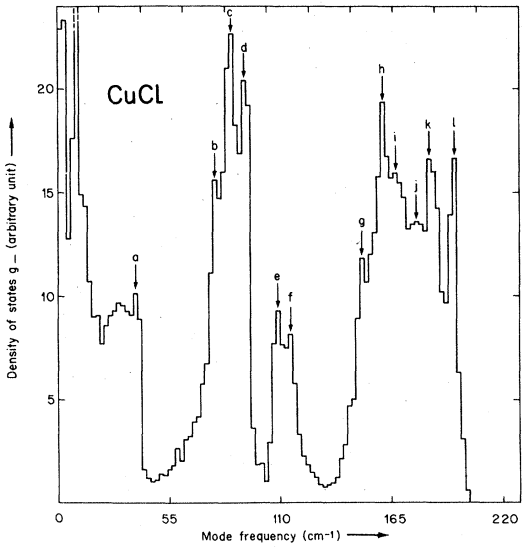

FIG. 7. The main peaks a, b, c, ..., e of two-phonon (subtractive) density of states (g_-) calculated by RIM 11 for CuCl are tentatively assigned using the selection rules of Birman (Ref. 40). Some of them may be compared with the two-phonon ir and Raman-scattering experimental data (Refs. 6, 10, and 12) (see Table III).

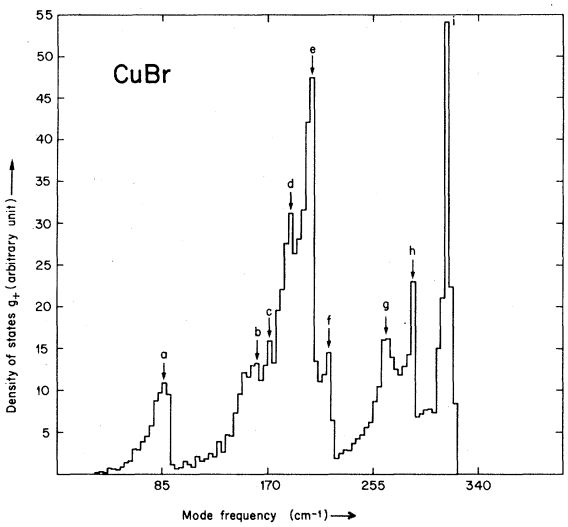

FIG. 8. Same key as Fig. 6 for CuBr. Some of the calculated peaks may be compared with the recent ir data of Maruyama *et al.*, Ref. 12 (see Table III).

able are insufficient to make a detailed analysis. Prevot *et al.*[6] have performed one- and two-phonon Raman-scattering experiments for CuCl at liquid-nitrogen temperature and have identified some of the features on the spectrum by pairs of phonons at high symmetric points. More recently Maruyama *et al.*[12] have measured ir absorption spectra of CuCl and CuBr at low temperatures (between 2-80 °K). They have noticed some discontinuity points in their absorption spectra on the low- and high-energy side of the TO band. By employing a more detailed analysis it has been

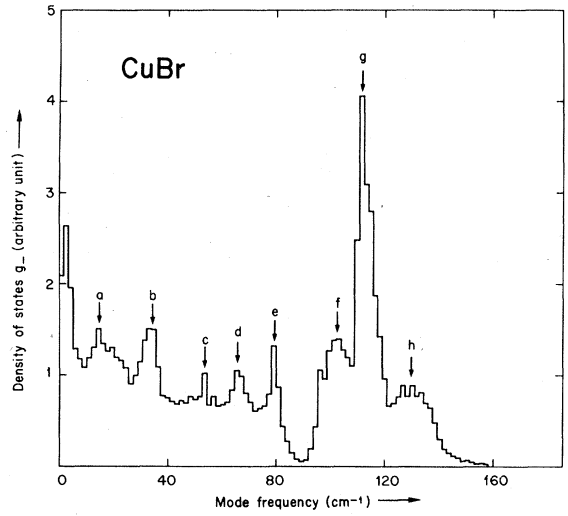

FIG. 9. Same key as Fig. 7 for CuBr. Some of the calculated peaks may be compared with the recent ir data of Maruyama *et al.*, Ref. 12 (see Table III).

TABLE III. Assignment of the main peaks calculated by one- and two-phonon density of states for CuCl and CuBr systems in units of cm^{-1}.

	CuCl							CuBr					
	g_+			g_-				g_+			g_-		
Peak	g	Calc.	Expt.	Assignment	Calc.	Expt.	Assignment	g	Calc.	Expt.	Assignment	Calc.	Expt.	Assignment
a	37.4	83	56[a]	2TA(*X*)	37	...	LO(*L*)-TO(*L*)	39	88	78[a]	2TA(*X*)	15	...	W_2-W_1
b	48	162	159 [b] 156[a]	LA(*X*)+TA(*X*)	79	78, [c] 78[a]	TO(*L*)-LA(*L*)	53	163	...	LA(*X*)+TA(*X*)	36		TO(*X*)-LA(*X*)
c	125	170	...	W_2+W_3	87	88[a]	LA(*L*)-TA(*L*)	118	173		TO(*L*)+TA(*L*)	56		LO(*L*)-LA(*L*)
d	210	254	...	TO(*X*)+TA(*X*)	94	100, [c] 95[a]	TO(*X*)-LA(*X*)	152	191		LO(*X*)+TA(*X*)	68	74[a]	W_3-W_2
e	233	270	274[a]	LO(*X*)+TA(*X*)	110	110, [c] 100[a]	LO(*X*)-LA(*X*)	172	208		W_6+W_1	81	88[a]	LA(*X*)-TA(*X*)
f		279	280[c]	LO(*L*)+TA(*L*)	116	105	LO(*L*)-LA(*L*)		221	217[a]	W_2+W_6	99	99[a]	W_4-W_2
g		345	336[a]	TO(*X*)+LA(*X*)	152	152[c]	?		269	270[a]	TO(*L*)+LA(*L*)	114	109[a]	LO(*X*)-TA(*X*)
h		357	360[c]	LO(*L*)+LA(*L*)	162	160[c]	TO(*L*)-TA(*L*)		289	290[a]	TO(*X*)+LA(*X*)	133		LO(*L*)-TA(*L*)
i		436	430, [c] 445[a]	LO(*L*)+TO(*Γ*)	168	166[c]	W_4-W_2 or W_5-W_2							or W_6-W_1
j				or 2TO(*X*)	179	176[c]	TO(*X*)-TA(*X*)		320	319[a]	LO(*L*)+TO(*L*)			
k					185	...	W_5-$W1$ or W_4-W_1				or 2TO(*X*)			
l					197	192[b]	LO(*X*)-TA(*X*)							
α	128							129						
β	167							136						

[a] Reference 12. [b] Reference 10. [c] Reference 6.

shown that phonon pairs at other than high symmetric points may generate many prominent Van Hove singularities on the two-phonon spectrum which can be interpreted only through a lattice-dynamical approach.[38]

In Table III, we have compared the main peaks in the calculated two-phonon density of states (sum and difference) with the corresponding temperature-dependent features observed in the experimental measurements for CuCl and CuBr. The data are analyzed in terms of phonons at Γ, X, L, and W critical points using the fact that the intensity of the difference ir bands approaches zero as $T \to 0$, whereas for the summation bands it decreases but remains nonzero even with $T \to 0$.[39] The analysis presented here is consistent with the polarization selection rules.[40]

C. Defect model

The mass-defect approximation (MDA) alone is insufficient in accounting for the restricted number of impurity vibrations (cf. Sec. II D). Among the possible 1-parameter defect models,[29,41] we consider the one which has already been applied to study the behavior of various point defects in several II-VI and III-V compounds.[30] An elaborate representation of the defect with more than one parameter will be meaningless owing to lack of experimental data for the present systems.

In our defect model, the only first neighbor short-range tensor force parameters A, B (diagonal and nondiagonal) of the perfect lattice are considered to be modified to A' and B' after perturbation by a substitutional impurity. Again we suppose that A' and B' are proportional to A and B, respectively, so as to describe the impurity by a single dimensionless parameter t as

$$t \equiv (A - A')/A = (B - B')/B \,. \tag{2}$$

This reduces the impurity space to a size of dimension 15×15 only. Again the group-theoretic arguments for the point-group symmetry $\{T_d\}$ further decomposes into irreducible subspaces of manageable sizes as

$$\Gamma_{T_d} = A_1 + E + F_1 + 3F_2 \,. \tag{3}$$

This model was proposed by Grimm *et al.*[41] for studying point defects in GaAs and has recently been applied for impurity vibrations of 63 substitutional defects in 9 II-VI and III-V compounds.[30] Considering experimental data as a probe the internal consistency of the model has been checked for several defect-host combinations. We have noticed that a single value of t explains two or even more different impurity modes observed recently by isoelectronic[38] and transition element impurities[42] in ZnS. In view of the above arguments the present study of defect vibrations in I-VII group is a logical extension of our earlier works. Again it is to be mentioned that in the F_2 modes and for the vibration of a very light substitutional atom in an otherwise frozen lattice, the recoil force (F) due to short-range interactions exerted on the impurity atom will be the sum of diagonal terms of the coupling matrices of nearest neighbor (A) and next-nearest neighbors (F_i and C_i) (Ref. 31, p. 389):

$$F = 4A' + 4F_i + 8C_i \quad (i = 1, 2) \,. \tag{4}$$

The localized mode frequency F_2 calculated in a simplified molecular approximation $[\omega_l = 2\pi (F/M_i')^{1/2}]$ will be independent of the term B. However, we find that the assumption that A' and B' vary in the same sense hardly affects the calculation of defect vibrations due to very light impurities. Finally we have not considered the change in long-range interactions for the present case of isoelectronic impurities, however, even for nonisoelectronic substituents the additional Coulombian interactions (for an F_2 mode of a very light impurity in a frozen lattice) are zero in the harmonic approximation.[43]

D. Localized gap and resonance modes

By incorporating the defect model (as described in Sec. II C) we have calculated the impurity mode frequencies in CuCl, CuBr, and CuI for different defect masses and different force constant perturbations t. In the actual numerical calculations the Green's functions were evaluated by summing over 16 369 uniformly distributed points in the reciprocal space and Eq. (1) was solved for t varying from $+1$ to -1. Only solutions of A_1 and F_2 symmetries were found. The results are displayed in Figs. 10–17. Using the experimental values of the local mode as a constraint we have estimated the force-constant changes incurred in various impurity-host systems. The results along with MDA calculations are summarized in Table IV.

A_1 modes. In the fully symmetric A_1 mode the substitutional site is immobile. The frequency of the mode is therefore independent of the impurity mass and is solely considered in terms of its interaction with the nearest-neighbor atoms. Our calculations show that this kind of localized "breathing mode" is possible for $t < -0.4$ and also when the immobile site of atom is of heavier mass (cf. Figs. 10, 15, and 17, e.g., in *Cu*Cl, Cu*Br*, and Cu*I*, respectively). However, the A_1 "breathing mode" in the gap region exists for the case when the immobile site of atom is of lighter mass, e.g., in Cu*Cl* (cf. Fig. 13). We feel that the defect bonding $t = -0.32$ established from the experi-

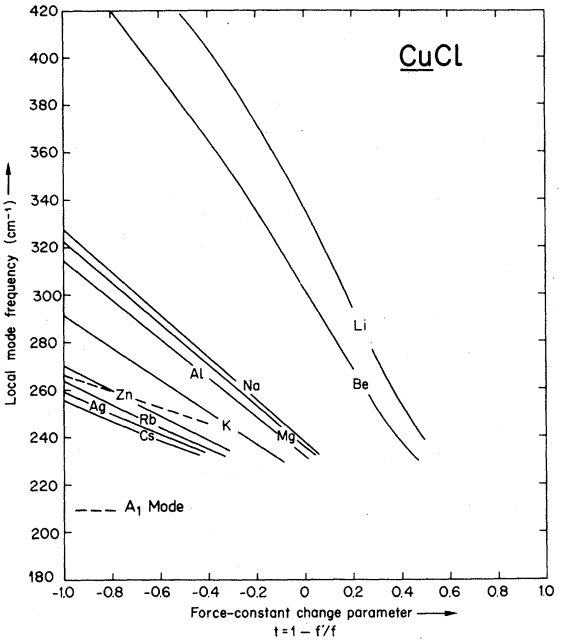

FIG. 10. *Cu*Cl: calculated frequencies of the F_2 localized mode for various substitutions on Cu site as a function of force-constant change parameter. The vibration of the A_1 mode is also shown as a dotted line.

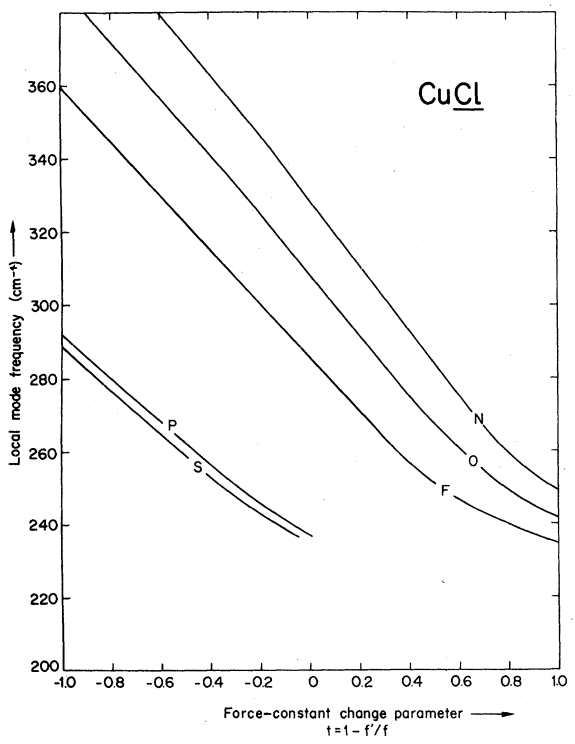

FIG. 11. Cu*Cl*: calculated frequencies of the F_2 localized mode for various substitutions on Cl site as a function of force-constant change parameter.

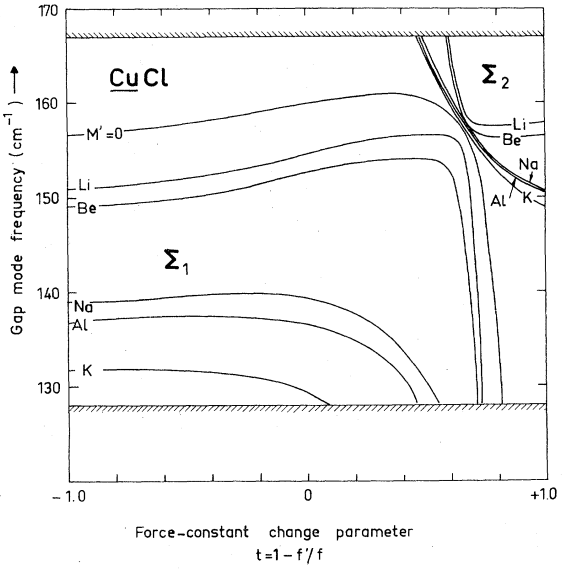

FIG. 12. *Cu*Cl: calculated frequencies of the F_2 gap mode for various substitutions on Cu site as a function of force-constant change parameter.

mentally known F_2 gap mode (148 cm^{-1}) of I impurity in Cu*Cl* should also give rise to a breathing mode with frequency 133 cm^{-1} in the gap region. Though the mode is Raman active, however, it has not been detected by Murahashi *et al.*[27] Finally we also find an in-band solution of Eq. (1) for the

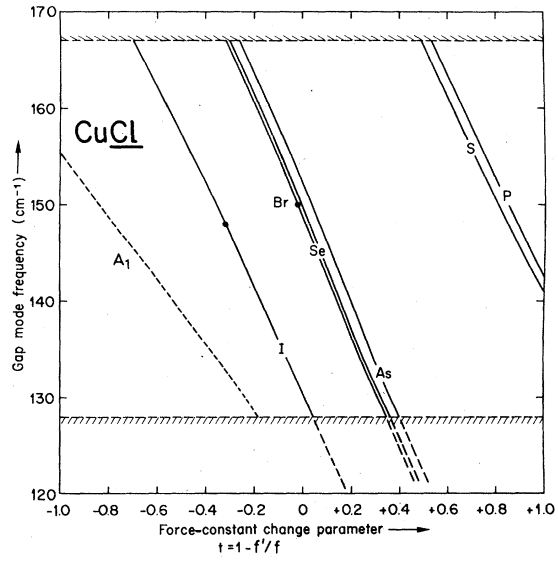

FIG. 13. Cu*Cl*: calculated frequencies of the F_2 gap mode for various substitutions on Cl site as a function of force-constant change parameter. Full dots (●) represent the experimental results of Murahashi and Koda (Ref. 27). The vibration of the A_1 mode is also shown as a dotted line.

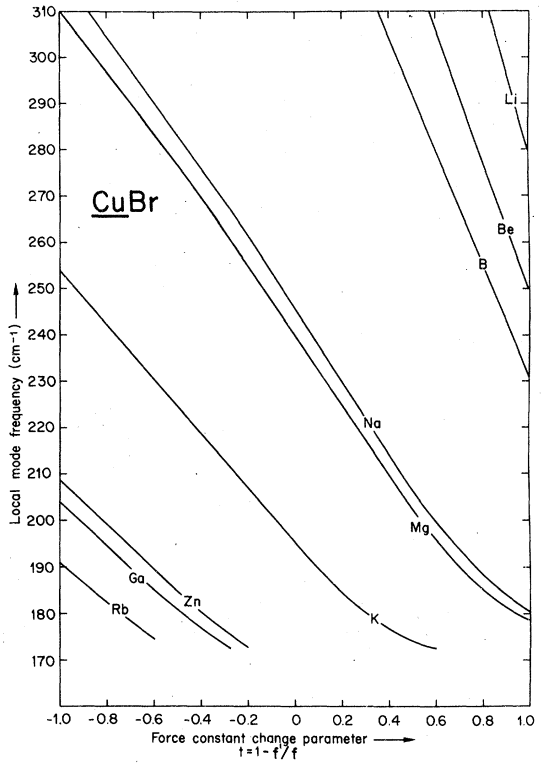

FIG. 14. *Cu*Br: calculated frequencies of the F_2 localized mode for various substitution on Cu site as a function of force-constant change parameter.

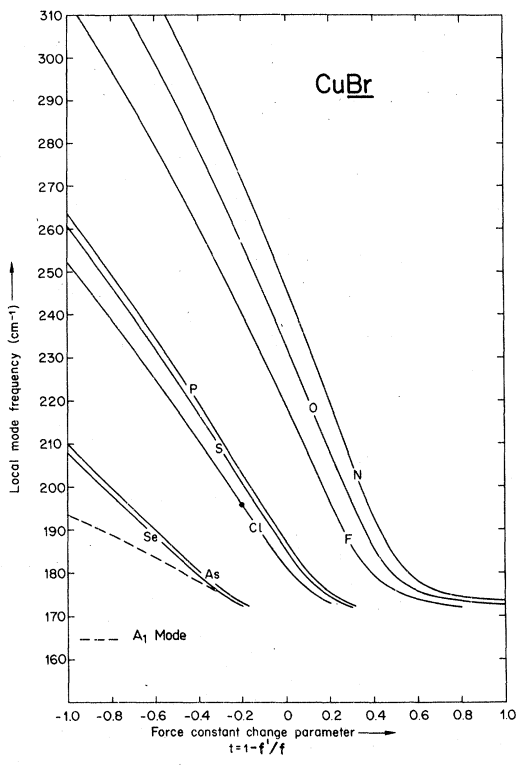

FIG. 15. Same key as Fig. 11 for Cu*Br*. The vibration of the A_1 mode is also shown as a dotted line. A full dot (●) represents the experimental results of Murahashi and Koda (Ref. 27).

A_1 vibrations of heavy atoms around the light immobile substituents, provided they are loosely bound to its neighbors ($t > 0.7$). These modes appear in the region of very weak density of states [Cu*Cl* (54 cm^{-1}), *Cu*Br (68 cm^{-1}), *CuI* (80 cm^{-1})] for $t = 1$ (vanishing bonding between defect and its first neighbors) and they should produce relatively narrow bands. As the frequency is independent of the impurity mass, the situation is probably close to that of an isolated vacancy (on Cl site in CuCl or on Cu site in CuBr and CuI, respectively). This suggests at least theoretically the possibility to study vacancy vibration by Raman-scattering technique.

F_2 modes. The triply degenerate F_2 modes are the most affected by any change of the parameters. Again these are the modes which are both ir and Raman active. We have paid special attention to the F_2 gap modes, as a simultaneous occurrence of both local and gap modes could provide an additional check of the adequacy for the defect

TABLE IV. Comparison of the calculated impurity modes with the available experimental data.

		Impurity mode frequency (cm^{-1})		
System	Mode	Expt.[a]	Calc. in MDA	Relative change in nearest-neighbor force constant $\Delta f/f = -t$
Cu*Cl*:Br	Gap	150	149	+0.02
Cu*Cl*:I	Gap	148	130.4	+0.32
Cu*Br*:Cl	Local	196	181.5	+0.20
Cu*I*:Cl	Local	186	177	+0.14

[a] Reference 27.

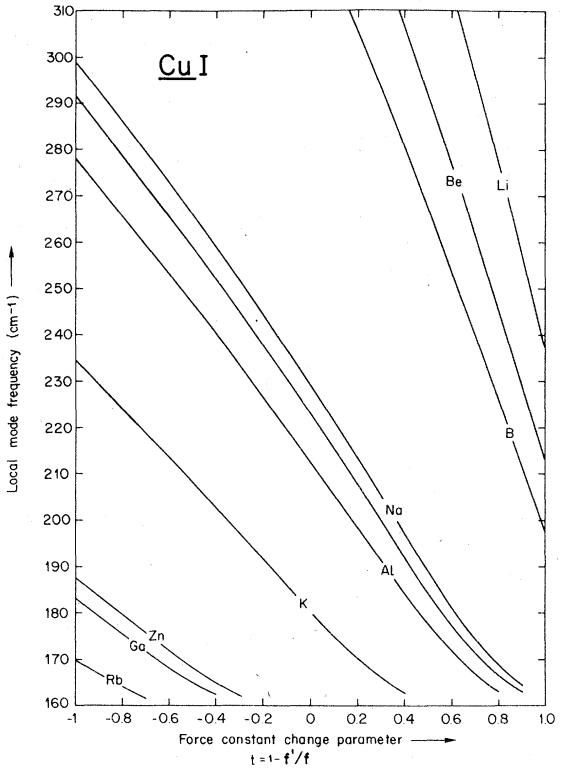

FIG. 16. *Cu*I: calculated frequencies of the F_2 localized mode for various substitutions on Cu site as a function of the force-constant change parameter.

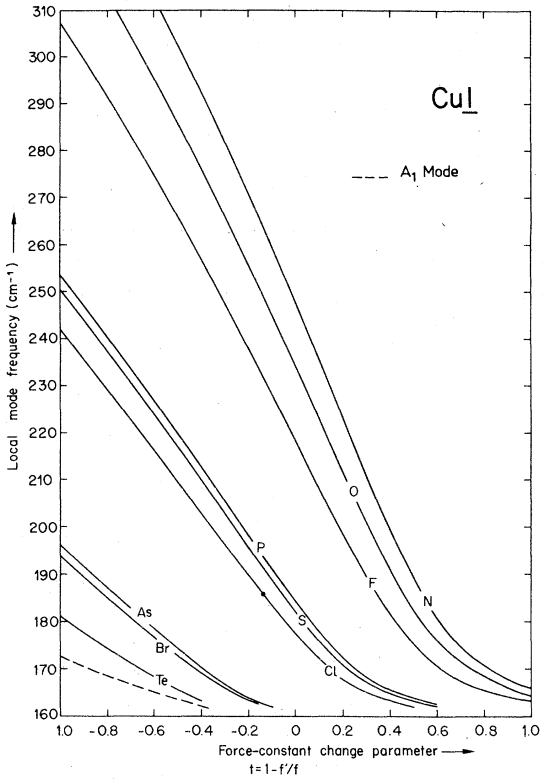

FIG. 17. Cu*I*: calculated frequencies of the F_2 localized mode for various substitutions on I site as a function of force-constant change parameter. The vibration of the A_1 mode is also shown as dotted line.

model in the I-VII case. In Fig. 12 we have plotted the calculated frequencies of the gap modes corresponding to various light atoms replacing Cu in CuCl. It is to be noted that for each light substituent we obtain two series of distinct curves Σ_1 and Σ_2 corresponding to two different states of the oscillating system. The Σ_2 series has not much physical significance as these modes only appear for t close to 1 (defects very loosely bound to their neighbors). On the other hand, the form of the Σ_1 curves represents a physical situation which is easy to explain: The large interval where the frequency of the gap mode is nearly independent of t corresponds to an almost rigid vibration of the impurity together with its four neighbors. This interval of perturbation ($t \lesssim 0.4$) provides an equal possibility for the occurrence of local modes due to light substitutional atoms on Cu sites in CuCl (Fig. 10); unfortunately, no experimental data are currently available in the literature. Again, we have also shown the results in the Σ_1 branch (cf. Fig. 12) for an impurity with zero mass. Since there does not exist a corresponding curve in the Σ_2 branch, it eliminates the possibility of detecting F_2 gap modes for isolated vacancies on Cu site in CuCl (tentatively: $M' \to 0$ and $t \to 1$).

There are fewer chances for the observation of gap modes in CuBr and CuI than in CuCl, principally because of their fairly narrow phonon gaps as noted in the one-phonon density of states (129 to 136 cm^{-1} in CuBr and 113 to 124 cm^{-1} in CuI, respectively). However, our calculations suggest the possibility of gap modes if impurities lighter than oxygen are substituted for Br in CuBr. One may also try to detect gap modes due to Cl impurities in Cu*I* for which we predict its possibility in the middle of the gap ($\simeq 119$ cm^{-1} for $t = -0.14$) on the basis of our localized mode calculation (Table IV).

Let us now examine solutions of Eq. (1) for the in-band modes of F_2 symmetry. These solutions can exist when the impurity is heavier than the substituted one (replacing Cl by Br and I impurities in Cu*Cl*). We do find band modes only in the region of weak phonon densities if they are very loosely bound to its neighbors, i.e., for $t \gtrsim 0.7$. This corresponds to an unphysical situation. These results are, in fact, the outcome of the

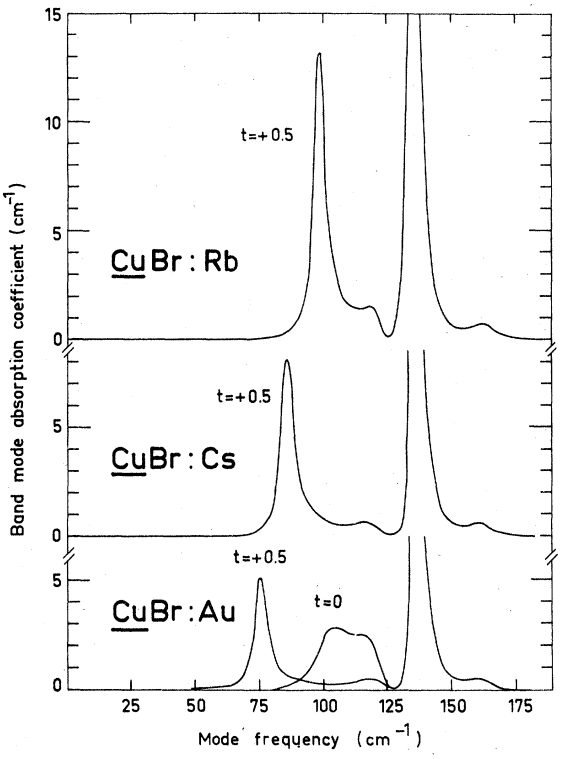

FIG. 18. Calculated band mode absorption coefficient for various impurities Rb, Cs, and Au (0.05 mol%) in *Cu*Br.

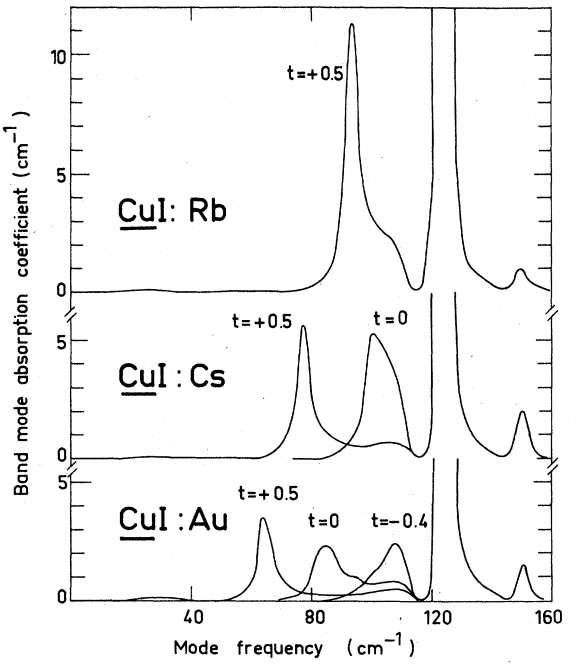

FIG. 19. Same key as Fig. 18 for *Cu*I.

graphical solution of Eq. (1) which have been extended (monotonically) to low-frequency regions (cf. Fig. 13). Since there exists a single $(\omega - t)$ curve per impurity vibration, only one impurity mode of this kind can exist in the plausible situation—and this is the gap mode which has been observed by Murahashi and Koda[27] for each of the Br and I impurities in Cu*Cl*. As no element with negative oxidation state heavier than iodine is available, the possible heavy substitution in Cu*Cl* is exhausted. The situation is, however, quite different for *Cu*Br and *Cu*I, as it is conceivable that the light atom could be replaced by very heavy mono or divalent atoms. Our calculations suggest that the in-band F_2 solutions of Eq. (1) in the region of low phonon density of states can be obtained for much more acceptable values of t.

The calculated coefficient of ir absorption (using the appendix) for some impurities in *Cu*Br and *Cu*I is displayed in Figs. 18 and 19 that once again requires its experimental verification. Finally the substitution on the Br and I sites in Cu*Br* and Cu*I* give rise to in-band modes only for $t \gtrsim 0.8$. This, as in the preceding case, does not correspond to any physically acceptable situation.

III. DISCUSSION

A perusal of Table IV reveals that the calculated impurity modes in the mass-defect approximation (MDA) are always lower than the experimental data and we require 2–32% stiffening in the nearest-neighbor interaction to achieve the observed values. The present results contradict the statement of Gaur *et al.*[44] that the force constants remain almost unchanged after perturbation due to isoelectronic impurities in zinc-blende–type crystals. Comparing the present results (Cu*I* : Cl, Cu*Br* : Cl) with the earlier calculations, we notice at first sight that the results are similar with II-VI (Cd*Te* : S) and III-V (In*Sb* : P) compounds where even more than 38% stiffening in nearest-neighbor interaction was estimated (cf. Table III, Ref. 30). Again, we have noticed that the ionic radii of the impurity and the host-lattice atom do not give any clue regarding the change of interaction. This statement in II-VI and III-V compounds is, in fact, the outcome of our results when compared with a large series of existing experimental data.

Although the impurity-host bonding (Cu-Br) in Cu*Cl* : Br is very close to that observed in perfect lattice CuBr, in three other cases (e.g., Cu-Cl in Cu*I* : Cl, Cu*Br* : Cl, and Cu-*I* in Cu*Cl* : I) it does not provide any correlation with the corresponding bond strength in their respective unperturbed

lattices (i.e., Cu-Cl in CuCl and Cu-I in CuI). However, our analysis for the gap mode frequencies due to *two* different impurities (Br and I) in *one* host system (CuCl) indicates that a few percent stiffening in force constant is required to obtain the experimental data for the gap mode due to Br impurities, and the stiffening increases to 32% when I impurities produce the gap mode in CuCl system. This trend of Br and I impurities in CuCl obtained from two distinct solutions using the same Green's functions (lattice phonons) suggests the possibility of the size effect—a behavior generally known for isoelectronic impurities in alkali halides.[26,45-47]

IV. CONCLUSION

It has been shown that the new low-temperature neutron data in cuprous halides can be well described by a simple rigid-ion model (RIM 11). We find that various substitutional impurities in cuprous halides may give rise to well-defined symmetry vibrations, both inside or outside the band mode region. The possibility is pointed out for some of the important cases to be observed through different (ir or Raman) experimental techniques. In the cases of known experimental data we have determined the force perturbation describing the impurity-host bonding in terms of a simple one-parameter model. The results are compared and discussed with our earlier results on II-VI and III-V compounds and also with the data available for alkali halides. It is to be noted from similar theoretical studies[29,30,41] that even if the absolute value of force variation due to impurities in ZBS compounds depends strongly on the lattice-dynamical model, however, their trend is found to be quite independent. We feel that the present *trend* of force variations will be reflected even with a more sophisticated lattice-dynamical model calculation; from two comparable cases (Cu*Cl* : Br and Cu*Cl* : I) it exhibits "size effect"—a behavior which is similar to alkali halides but is different from other ZBS compounds. The statistics currently available are rather incomplete and cannot be generalized for all isoelectronic impurities in cuprous halides unless more experimental results are known.

ACKNOWLEDGMENT

We are thankful to Dr. S. Hoshino for sending us their detailed neutronic results for CuBr system. One of us (D.N.T.) is thankful to the Commissariat a l'Energie Atomique (CEA) authorities for providing him an opportunity as a collaborator in "Services d'Electronique de Saclay."

APPENDIX: IMPURITY-INDUCED ir ABSORPTION IN ZBS CRYSTALS

The Green's-function theory for the impurity-induced ir absorption due to point defects in polar crystals has been discussed in several monographs.[31,45-47] The extension of the theory to ZBS crystals by one of the authors[48] provides good results in the MDA, however, they need some rectification for including the force-constant changes. The treatment to be presented here is exactly followed from that of Klein,[45] with the notations of Maradudin,[31(a)-31(c)] in particular, with the same definition of phonon and Green's functions.

In the harmonic approximation, the absorption coefficient due to a single impurity is given by[48]

$$\alpha(\omega) = \frac{4\pi\omega}{9Nv_0c}\,\frac{(n_\infty^2+2)^2}{n(\omega)}\,\frac{e^{*2}}{\mu} \times \mathrm{Im}\langle 0, \mathrm{TO}_1|M^{1/2}gtgM^{1/2}|0, \mathrm{TO}_1\rangle\,, \tag{A1}$$

where n_∞^2 is the high-frequency dielectric constant, $n^2(\omega)$ is the dielectric constant at frequency ω, c is the velocity of light, N is the number of unit cells in the crystal, v_0 is the volume of a unit cell of reduced mass μ, e^* is the effective charge (taken as Szigetti's effective charge), M is the diagonal matrix containing the masses of the constituent atoms, and $|0, \mathrm{TO}_1\rangle$ is one of the normalized eigenvectors $|\vec{q}, j\rangle$ with $\vec{q}=0$ and $j=\mathrm{TO}_1$, i.e., the transverse optical phonon polarized in the 1-direction. The t matrix is related to the Green's-function matrix for the perfect lattice (g) and the perturbation matrix (δl) as

$$t = \delta l(I - g\delta l)^{-1}. \tag{A2}$$

Again the vector $|0, \mathrm{TO}_1\rangle$ diagonalizes the Green's-function matrix, i.e.,

$$g|0, \mathrm{TO}_1\rangle = M^{-1}(z-\omega_{\mathrm{TO}}^2)^{-1}|0, \mathrm{TO}_1\rangle\,, \tag{A3}$$

where ω_{TO} is the $\vec{q}=0$, TO-phonon frequency and $z=\omega^2-i\epsilon$.

The problem of local perturbation due to an isolated defect can be simplified with the help of symmetry vectors (Γi), where Γ is the irreducible representation of the point group pertaining to the perturbation and i runs from one to the number of times $[n(\Gamma)]$ the irreducible representation Γ is contained in the perturbation. The squared matrix $(\Gamma i|lk\alpha)$, where the indices $l\alpha$ and α are now restricted to the perturbation subspace, represents the unitary transformation from the subspace of Cartesian coordinates to that of the symmetry coordinates. Thus the projected Green's-function matrix of the perfect lattice associated with the irreducible representation (Γ)

may be written as

$$(\Gamma i|g|\Gamma i') = \sum_{\vec{q}j} \frac{(\Gamma i|\vec{q}j)(\vec{q}j|\Gamma i')}{z-\omega^2(\vec{q},j)} ,$$

with

$$(\Gamma i|\vec{q}j) = \sum_{lk\alpha} (\Gamma i|lk\alpha)(lk\alpha|\vec{q}j)$$

$$= \sum_{lk\alpha} (\Gamma i|lk\alpha) e_\alpha(k|\vec{q}j) , \qquad \text{(A4)}$$

l denotes the unit cell, k corresponds to the type of atoms in it, and $e_\alpha(k|\vec{q}j)$ is the αth component of the polarization vector of the phonon with wave vector $\vec{q}$ and branch index j. Using the symmetry coordinates for the F_2 irreducible representation[49] and the properties of the polarization vectors[45] one may obtain

$$(F_2 i=1|0,\mathrm{TO}_1) = \delta_{ii'} e_{i'}(\pm|0,\mathrm{TO}_1) = \left(\frac{\mu}{M_\pm}\right)^{1/2} \delta_{ii'} ,$$

$$(F_2 i=2|0,\mathrm{TO}_1) = 2\delta_{ii'} e_{i'}(\mp|0,\mathrm{TO}_1) = -2\left(\frac{\mu}{M_\mp}\right)^{1/2} \delta_{ii'} , \qquad \text{(A5)}$$

and

$$(F_2 i=3|0,\mathrm{TO}_1) = 0 .$$

The $(\pm)$ sign on $M_\pm$ denotes the mass of the positively or negatively charged ion, respectively. The upper (lower) sign is taken if the impurity atom is considered on the (+) (−) ion site.

Using (A3) and (A5) the expression for ir absorption due to a random distribution of impurity ions with a fractional concentration p is finally written as

$$\alpha(\omega) = \frac{4\pi e^{*2}}{9 v_0 c} \frac{(n_\infty^2+2)^2}{n(\omega)} \frac{\omega}{(\omega^2-\omega_{\mathrm{TO}}^2)^2} \frac{p}{\mu} \mathrm{Im} t_{00}(z) , \qquad \text{(A6)}$$

where $t_{00}(z)$ is the matrix element of the t matrix in F_2 irreducible representation for $\vec{q}=0$, TO phonon and is given by

$$t_{00}(z) = \mu\left(\frac{t_{11}}{M_\pm^2} - \frac{4t_{12}}{M_\pm M_\mp} + \frac{4t_{22}}{M_\mp^2}\right) \qquad \text{(A7)}$$

for ZBS crystals. It comes out from Eq. (A7) that the $t_{i3}=t_{3i}$ elements of the symmetric t matrix is zero (for $i=1,2,3$). This is related to the fact that the dipole moment induced by one of the allowed movements in F_2 mode is zero[49] [see Eq. (A5)].

---

*Visiting scientist. Permanent address: Department of Physics, University of Allahabad, Allahabad, 211002, India.

†Present address: Xerox Corporation, Palo Alto Research Center, 3333 Coyote Hill Road, Palo Alto, California 94304.

[1]S. Iwasa and E. Burstein, J. Phys. (Paris) 26, 614 (1965).

[2]M. A. Nusimovici and A. Meskaoui, Phys. Status Solidi B62, K69 (1972).

[3]B. Prevot, C. Carabatos, and M. Leroy, C. R. Acad. Sci. 274, 707 (1972).

[4]I. M. Kaminow and E. H. Turner, Phys. Rev. B 5, 1564 (1972).

[5]T. Fukumota, K. Tabuchi, S. Nakashima, and A. Mitsuishi, J. Phys. Soc. Jpn. 35, 622 (1973).

[6]B. Prevot and M. Sieskind, Phys. Status Solidi B59, 133 (1973).

[7]J. E. Potts, R. C. Hanson, C. T. Walker, and C. Schwab, Phys. Rev. B 9, 2711 (1974); Solid State Commun. 13, 389 (1973).

[8]M. Krauzman, R. M. Pick, H. Poulet, G. Hamel, and B. Prevot, Phys. Rev. Lett. 33, 528 (1974).

[9]J. M. Plendl, A. Hadni, J. Claudel, Y. Henninger, G. Morlot, P. Strimer, and L. C. Mansur, Appl. Opt. 5, 397 (1966).

[10]A. Hadni, F. Brehat, J. Claudel, and P. Strimer, J. Chem. Phys. 49, 471 (1968).

[11]J. N. Plendl and L. C. Mansur, Appl. Opt. 11, 1194 (1972).

[12]M. Maruyama, T. Naba, and M. Ikezawa, J. Phys. Soc. Jpn. 42, 1789 (1977); 44, 1231 (1978).

[13]C. Carabatos, B. Hennion, K. Kunc, F. Moussa, and C. Schwab, Phys. Rev. Lett. 26, 770 (1971).

[14]B. Hennion, F. Moussa, B. Prevot, C. Carabatos, and C. Schwab, Phys. Rev. Lett. 28, 964 (1972).

[15]B. Prevot, C. Carabatos, C. Schwab, B. Hennion, and F. Moussa, Solid State Commun. 13, 1725 (1973).

[16]S. Hoshino, Y. Fujii, J. Harada, and J. D. Axe, J. Phys. Soc. Jpn. 41, 965 (1976).

[17]B. Prevot, B. Hennion, and B. Dorners, J. Phys. C 10, 3999 (1977).

[18]D. Chemla, P. Kupecek, C. Schwartz, C. Schwab, and A. Goltzene, IEEE J. Quantum Electron. QE-7, 126 (1971).

[19]E. H. Turner, I. P. Kaminow, and C. Schwab, Phys. Rev. B 9, 2524 (1974).

[20]Z. Vardeny, D. Moses, G. Gilat, and H. Shechter, Solid State Commun. 18, 1369 (1976); Phys. Rev. B 11, 5175 (1975).

[21]T. H. K. Barron, J. A. Birch, and G. K. White, J. Phys. C 10, 1617 (1977).

[22]S. Miyake, S. Hoshino, and T. Takenaka, J. Phys. Soc. Jpn. 7, 19 (1952).

[23]S. Hoshino, J. Phys. Soc. Jpn. 7, 560 (1952).

[24]S. Miyake and S. Hoshino, Rev. Mod. Phys. 30, 172 (1958).

[25]J. Harada, H. Suzuki, and S. Hoshino, J. Phys. Soc. Jpn. 41, 1707 (1976).

[26]J. C. Phillips, Rev. Mod. Phys. 42, 317 (1970).

[27]T. Murahashi and T. Koda, J. Phys. Soc. Jpn. 40, 747 (1976).

[28]G. Benedek and G. F. Nardelli, Phys. Rev. 155, 1004 (1961).
[29]D. N. Talwar and Bal K. Agrawal, Phys. Rev. B 12, 1432 (1975).
[30]M. Vandevyver and P. Plumelle, Phys. Rev. B 17, 675 (1978).
[31](a) A. A. Maradudin, E. W. Montroll, G. H. Weiss, and I. P. Ipatova, *Solid State Physics*, Suppl. 3, 2nd ed. (Academic, New York, 1971). (b) A. A. Maradudin, in *Astrophysics and Many Body Problems*, 1962 Brandeis Lectures (Benjamin, New York, 1963). (c) A. A. Maradudin, *Solid State Physics* (Academic, New York, 1966), Vols. 18 and 19. (d) A. A. Maradudin, Rep. Progr. Phys. 28, 331 (1965).
[32]K.Kunc, Ann. Phys. (Paris) B 319 (1973–74).
[33]We call *homogeneous* such a set of models in which parameters of "related" compounds are related. This means, in particular, the following: (a) In every isoelectronic series (II-VI, III-V, etc.) the first-neighbor interaction parameters are slowly varying functions of interatomic distance. (b) Two compounds differing by only cation have nearly identical force constants (e.g., InSb and GaSb or ZnTe and CdTe). (c) Model parameters of any compound can be approximately obtained by averaging parameters of the two compounds with the same cation and with anions of adjacent iso-column [e.g., $ZnSe \leftarrow \frac{1}{2}(ZnS + ZnTe)$]. (d) Model parameters of III-V or II-VI compounds can be related to those of the "closest" II-VI or III-V compounds by a constant factor (e.g., $ZnTe \rightleftarrows GaSb$, etc.). For more detailed discussion and illustrated examples, we refer to some recent articles (Refs. 34–36). It is worth mentioning for future studies that the overlap valence shell model (OVSM) may provide a *homogeneous* set of parameters too (Refs. 35 and 36). Again the related data are either unpublished or appeared very recently and, in particular, the results for cuprous halides are still missing.
[34]K. Kunc and H. Bilz, in *Proceedings of the Conference on Neutron Scattering, Gallinburg*, 1976, edited by R. M. Moon (ORNL, Oak Ridge, Tenn., 1976), p. 195.
[35]P. Borcherds and K. Kunc, J. Phys. C 11, 4145 (1978).
[36]N. Meskini and K. Kunc (unpublished).
[37]P. Plumelle and M. Vandevyver, Phys. Status Solidi B73, 271 (1976).
[38]M. Vandevyver and P. Prumelle, J. Phys. Chem. Solids 38, 765 (1977).
[39]J. N. Hodgson, *Optical Absorption and Dispersion in Solids*, J. N. Hodgson (Chapman and Hall, London, 1970), p. 40.
[40]J. L. Birman, Phys. Rev. 131, 1489 (1963).
[41]A. Grimm, A. A. Maradudin, I. P. Ipatova, and A. V. Subashiev, J. Phys. Chem. Solids 33, 775 (1972); A. Grimm, in *Lattice defects in Semiconductor 1974, Conference Series N 23*, edited by A. Seeger (Institute of Physics, London, 1975), p. 332.
[42]M. Zigone, K. Kunc, P. Plumelle, and M. Vandevyver, in *Proceedings of the International Conference on Lattice Dynamics, Paris*, 1977, edited by M. Balkanski, p. 405.
[43]E. W. Kellerman, Philos. Trans. R. Soc. London A 230, 513 (1970).
[44]S. P. Gaur, J. F. Vetelino, and S. S. Mitra, J. Phys. Chem. Solids 32, 2737 (1971).
[45]M. V. Klein, in *Physics of Color Centres*, edited by W. G. Fowler (Academic, New York, 1968), Chap. 7, p. 429.
[46]A. S. Barker and A. J. Sievers, Rev. Mod. Phys. 47, Suppl. 2 (1975), and references cited therein.
[47]T. P. Martin, Phys. Rev. 160, 686 (1967).
[48]D. N. Talwar and Bal K. Agrawal, Phys. Rev. B 9, 4362 (1974).
[49]W. Ludwig, in *Ergebnisse der Exakren Naturwissenshaften*, edited by S. Flugge and F. Trendelenburg (Springer, Berlin, 1964), Vol. 33, p. 1.